

## Profile cone penetrometer data used to distinguish between soil materials

S. Grunwald<sup>a,\*</sup>, B. Lowery<sup>a</sup>, D.J. Rooney<sup>b</sup>, K. McSweeney<sup>a</sup>

<sup>a</sup>Department of Soil Science, University of Wisconsin–Madison, 263 Soils Building, 1525 Observatory Drive, Madison, WI 53706-1299, USA

<sup>b</sup>Environmental Remote Sensing Center, University of Wisconsin–Madison, 1225 W. Dayton Street, Madison, WI 53706, USA

Received 21 November 2000; received in revised form 11 April 2001; accepted 12 April 2001

### Abstract

In young glaciated landscapes the variability of soil materials imparts a major control on crop growth and yield and environmental quality associated with production agriculture. Two common soil materials found on these glaciated landscapes are glacial till and reworked loess. Soil materials can be characterized by a combination of physical and morphological soil attributes. We hypothesized that penetration resistance is the response signal to a complex of multiple soil attributes and can be used as an integrating indicator to map soil materials. Our objective was to test the ability of a profile cone penetrometer to map soil materials at landscape-scale. The study site was located in southern Wisconsin, USA, on soils developed in reworked loess material overlying glacial till, which are classified as Typic or Mollic Hapludalfs and Typic Argiudolls. We collected a dense data set of cone index profiles from a 2.73 ha area on a 10 m grid up to depths of 1.3 m. Additionally, we collected soil cores randomly at 21 penetration locations and analyzed these by layer for texture, bulk density, and water content. We utilized point elevation data collected with a differential global positioning system to create a digital elevation model and derive slope and compound topographic index to subdivide the study area into landform element classes. We used expert knowledge to characterize soil materials and subsequently measured soil attributes to identify soil materials. A hierarchical cluster analysis was used to group cone index profiles. Combining the sparse soil material data with the dense cone index and landform element data resulted in soil material information covering the entire study area. The spatial distribution of soil materials was visualized using a three-dimensional soil layer model. The proposed method is associated with large uncertainties in some areas and can be recommended only for coarse mapping of contrasting soil materials such as glacial till and reworked loess at landscape-scale, when used in combination with landform element data. © 2001 Elsevier Science B.V. All rights reserved.

*Keywords:* Penetration resistance; Cone index; Soil materials; Landscape approach; Bulk density; Texture; Water content

### 1. Introduction

#### *1.1. Soil materials in young glaciated landscapes*

In young glaciated landscapes (Wisconsin-age, <15,000 YBP), featuring restricted and immature drainage networks, soil landscape variability imparts a major control on productivity and environmental

\*Corresponding author. Present address: Assistant Professor Land Resources, Soil and Water Science Department, University of Florida, 2171 McCarty Hall, P.O. Box 110290, Gainesville, FL 32611, USA. Tel.: +1-352-331-8538; fax: +1-352-392-3902. E-mail address: sgrunwald@mail.ifas.ufl.edu (S. Grunwald).

quality associated with production agriculture. Besides gently rolling to level topography, climate, and tillage practices, soil material is a dominant factor influencing crop growth and yield and the fate and transport of agrichemicals. Two common soil materials found in glaciated landscapes are glacial till and reworked loess. Glacial till is unsorted and unstratified material deposited by glacial ice. In southern Wisconsin, USA, the till consists mainly of sand, loam, gravel, and stones in various proportions. This sand rich material has large bulk density and penetration resistance and limited macroporosity. This results mainly from structural failure (collapse) of soils having low-stability aggregates. Awadhwai and Smith (1990) showed that Alfisols with high sand content are especially prone to develop a dense zone with high penetration resistance.

Another soil material commonly found in young glaciated landscapes is loess, which is material transported and deposited by wind. Since loess was deposited it has been subjected to a variety of processes such as erosion, deposition, and decalcification. Thus, it is denoted as 'reworked loess'. According to the Soil Survey of Columbia County, which describes soil patterns of the area investigated in this study, reworked loess material consists mainly of silt loam, silty clay loam, and loam with medium bulk densities. Assallay et al. (1998) indicate that fragipans or dense subsurface horizons might develop in soils formed in loess, which are subsurface horizons with high bulk density and/or high penetration resistance that are very hard when dry, but showing a moderate to weak brittleness when moist. According to the hydroconsolidation hypothesis, fragipans develop because of structural collapse favorably in soils with: (i) clay contents between 5 and 30%, (ii) an overburden pressure to produce enough compressive stress where significant collapse occurs under stresses of >200 kPa, and (iii) sufficient water content to allow the hydroconsolidation process to occur (Assallay et al., 1998).

Glacial till and reworked loess soil materials differ across the landscape in a variety of soil characteristics such as compaction, texture, water holding capacity, structure, porosity, drainage, adsorptivity, and leaching of agrichemicals. These differences greatly affect soil management especially tillage, fertilization needs, and crop yield.

### *1.2. Relationship between soil properties and penetration resistance*

Among the soil characteristics that influence penetration resistance are texture, porosity, structure, water content, cementing agents, and compaction. Correlations between particle size and penetration resistance were presented by Kasim et al. (1986), Kurup et al. (1994), and Puppala et al. (1995), where coarse textured soils showed greater penetration resistance when compared to fine textured soils. Water content is inversely related to penetration resistance (Ayers and Perumpral, 1982). Faure and Da Mata (1994) found that penetration resistance was very low, or close to zero, when water contents were very large, especially, when the soil was nearly saturated. For any soil at a given bulk density, penetration resistance decreased as water content increased (Bar-Josef and Lambert, 1981; Laboski et al., 1998). Penetration resistance is bound to increase with cementation due to the effect of cementing agents such as carbonate, silica, hydrous silicate, and hydrous iron oxide (Puppala et al., 1995). Lowery and Schuler (1994) showed that penetration resistance and bulk density increased with increasing levels of compaction.

Tillage influences penetration resistance indirectly. Taboada et al. (1998) demonstrated that zero tillage increased penetration resistance significantly in a sandy loam from 0.8 to 5.0 MPa and in a silty clay loam from 1.9 to 3.2 MPa, which were attributed to soil hardening. No-tillage with residues, no-tillage after wheat, and conventional tillage after sorghum under controlled traffic conditions did not significantly affect penetration resistance, bulk density, and water content (Unger, 1996). Subsoiling effects on a sandy loam and its impact on penetration resistances was tested by Pikul and Aase (1999) resulting in smaller penetration resistance of 891 kPa averaged over a 2.5-year period on subsoiled plots using a paratill and higher penetration resistance of 981 kPa on plots without subsoiling. Materechera and Mloza-Banda (1997) showed that penetration resistance was significantly higher for minimum ridge-tillage system when compared to conventional tillage. Negative correlations between penetration resistance and crop growth were shown by Bowen (1976), Voorhees (1987), and Trowse (1983).

Penetration resistance measurements are influenced by a variety of permanent and dynamic soil properties such as texture, bulk density, and water content. Results of numerous research studies suggest that soil properties impact penetration resistance, however, most researchers have not quantified the contribution of specific soil properties on penetration resistance.

### 1.3. Soil materials and penetration resistance

We hypothesize that soil material can be characterized by a combination of morphological and physical soil properties based on expert knowledge, which can be expressed as

$$\text{Isoma}_{xyz,t} \Leftrightarrow \text{texture}_{xyz,t}; \text{bulkdensity}_{xyz,t}; \text{watercontent}_{xyz,t}; \text{sopr}_{xyz,t}$$

where

$\text{Isoma}_{xyz,t}$ : Soil material at a geographic location  $x$  and  $y$ , depth  $z$  in m, and time  $t$ .

$\text{texture}_{xyz,t}$ : Texture at a geographic location  $x$  and  $y$ , depth  $z$  in m, and time  $t$  with:

- sand content — minimum, maximum, or range in %
- silt content — minimum, maximum, or range in %
- clay content — minimum, maximum, or range in %

$\text{bulkdensity}_{xyz,t}$ : Bulk density at a geographic location  $x$  and  $y$ , depth  $z$  in m, and time  $t$  with: minimum, maximum, or range in  $\text{Mg m}^{-3}$

$\text{watercontent}_{xyz,t}$ : Water content at a geographic location  $x$  and  $y$ , depth  $z$  in m, and time  $t$  with: minimum, maximum, or range in  $\text{m}^3 \text{m}^{-3}$

$\text{sopr}_{xyz,t}$ : Other soil properties at geographic location  $x$  and  $y$ , depth  $z$  in m, and time  $t$ .

Cone index (CI) is defined as the force per unit basal area required to push a profile cone penetrometer (PCP) through a specified increment of soil. CI corresponds

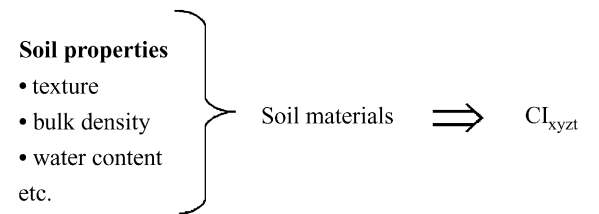
to penetration resistance measured at a specific location and a specific time, which can be expressed as

$$\text{CI}_{xyz,t}$$

where

- CI: Cone index (kPa)
- $x$ : Geographic coordinate  $x$
- $y$ : Geographic coordinate  $y$
- $z$ : Depth (m), and
- $t$ : Time.

Penetration resistance is the response signal to a complex of multiple soil properties. A combination of specific soil properties characterizes soil materials such as glacial till and reworked loess. We hypothesize that penetration resistance is a surrogate for soil material:



Based on these hypotheses the objective of this study was to test the ability of a PCP to distinguish among soil materials found in a glaciated landscape of southern Wisconsin. We used the PCP as a tool to map soil material at landscape-scale.

## 2. Methods

### 2.1. Data collection

The methodological steps for data collection, analyses, and visualization is shown in Fig. 1. We used a constant rate PCP with a cone tip angle of  $60^\circ$  and a 2 cm diameter surface area to measure CI. The PCP system components included the PCP probe, a hydraulic truck mounted push system (Gidding #9HD; Fort Collins, CO),<sup>1</sup> a load cell (1360 kg capacity; Omega-dyne LC 101; Sunbury, OH), a depth transducer

<sup>1</sup>Mention of company or trade name does not constitute endorsement by the University of Wisconsin–Madison or the authors.

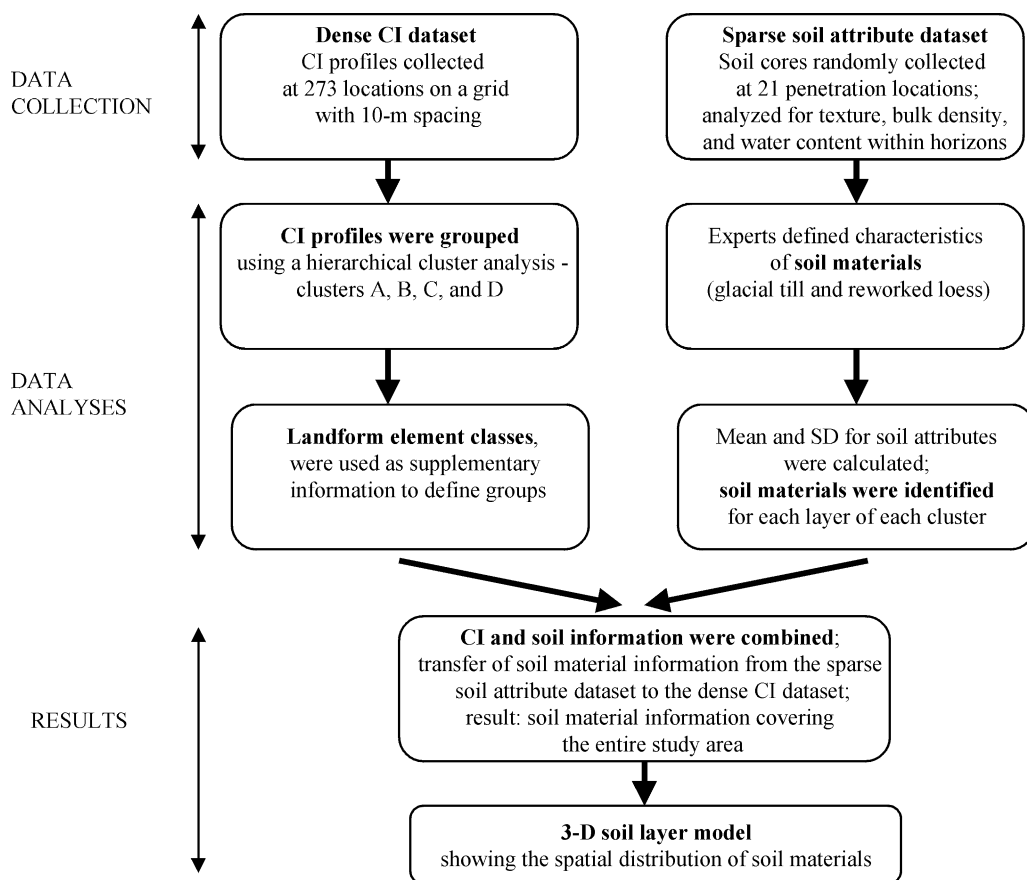


Fig. 1. Methodological steps for data collection, analysis, and visualization.

(Unimeasure HX-EP; Corvallis, OR), and a data acquisition system (datalogger, Campbell Scientific 21X; Logan, UT). This system was described by Rooney and Lowery (2000). CI measurements were made to a depth of 1.30 m with values being recorded at average depth increments of 0.5 cm. A cone index profile (CIP) was obtained for each location on a  $10 \times 10$  m grid covering an area of 2.73 ha resulting in 273 penetration profiles denoted as 'dense CI data set'. Our objective was to map soil materials, therefore, we did not sample furrow and row positions separately. Each record of the dense CI data set consisted of CI values, position coordinates  $x$  and  $y$ , depth in meters, and time of measurement.

We used a Trimble 4600 LS differential global positioning system (dGPS), single frequency, dual port, with an internal 4600 LS antenna (Trimble,

1996; Sunnyvale, CA) and Beacon correction to georeference sampling locations with a horizontal resolution error  $\pm 4$  cm. Additionally, we used the dGPS unit to conduct a kinematic survey to derive a digital elevation model (DEM) for the study area. A grid-size of 1 m was chosen utilizing inverse distance method for interpolation of point elevations.

To characterize soil materials we collected randomly soil cores at 21 penetration locations denoted as 'the soil attribute data set'. Penetrations and soil coring was done quasi-simultaneously (within 1–2 h time frame). We analyzed horizons of cores for texture, bulk density ( $\rho_b$ ), and water content ( $\theta$ ). Soil texture was analyzed by the University of Wisconsin–Madison Soil and Plant Analyses Laboratory (Madison, WI) using the hydrometer method. We obtained water content data by collecting known volumes of

samples and oven drying them to obtain volumetric values. We determined bulk density on a dry weight basis from the same samples used for water content determinations.

## 2.2. Data analysis of topographic attributes

We used the ArcView GIS 3.0 (ArcView, 1999) to derive slope and compound topographic index (CTI). CTI is a simplified measure to describe the spatial distribution of water flow across a study area (Beven and Moore, 1993) and is calculated as follows:

$$w = \ln\left(\frac{a}{\tan \beta}\right)$$

where  $w$  is the CTI,  $a$  the cumulative upslope area draining through a point (per unit contour length), and  $\tan \beta$  the slope angle at that point.

The CTI reflects the tendency of water to accumulate at any point in the watershed (in terms of  $a$ ) and the tendency for gravitational forces to move that water downslope (expressed in terms of  $\tan \beta$ ) as an approximate hydraulic gradient.

Elevation, slope, and CTI were used to identify landform elements according to the classification scheme developed by Huggett (1975) (Table 1). Landform elements describe the location of a specific sampling point within a landscape, i.e., the geographic  $x$  and  $y$  coordinates.

Table 1  
Landform element classes for our study area according to Huggett (1975)

| Landform elements <sup>a</sup> | Topographic attributes |           |         |
|--------------------------------|------------------------|-----------|---------|
|                                | Elevation (m)          | Slope (°) | CTI (–) |
| Toeslope                       | 321–323                | <1.5      | >8      |
| Footslope                      | 323–325                | 1.5–2.5   | 6–8     |
| Backslope                      | 325–327                | 2.5–8.0   | 6–4     |
| Shoulder                       | 327–328                | 2.0–4.0   | 4–2     |
| Summit                         | 328–329                | <2.0      | <2      |

<sup>a</sup> Toeslope: the region which extends away from the base of the hillslope (depositional area); footslope: the concave part of the hillslope (depositional area); backslope: steepest slope gradient of the hillslope; shoulder: the convex component between the summit and the backslope; summit: an upland surface with an inclination, which differs distinctly from the hillslope which ascends to it.

## 2.3. Data analysis of cone indices

We used a hierarchical cluster method to group similar penetrations into clusters, i.e., penetrations which showed a similar CIP were classified into the same cluster. First, we removed noise from the PCP data set, which occurred in some penetrations because stones were encountered. While encountering stones CI increased sharply with a rate  $>300 \text{ kPa cm}^{-1}$ . Thus, a smoothing technique was used to remove noise. We averaged CI for 3 cm depth increments along each profile to standardize CI. This was a necessary step to conduct the hierarchical cluster analysis to form groups of similar penetrations. The key measure in cluster analysis is ‘similarity’ which measures closeness. In general, similarity measures are large indicating strong similarity and small indicating little similarity. The Pearson correlation coefficient ( $r$ ) is one of the most frequently used measures of similarity between two variables (SPSS Professional Statistics, 1994). We used ‘average linkage within groups’ to combine clusters. This method combines clusters so that the average distance between all cases in the resulting cluster is as small as possible. Thus, the distance between two clusters is taken to be the average of the distances between all possible pairs of cases in the resulting cluster. We used the Pearson correlation coefficient to test similarity between variables. In agglomerative hierarchical clustering, clusters are formed by grouping cases into bigger and bigger clusters until all individuals are members of a single cluster. The agglomeration schedule and dendrogram can be used to follow up the grouping process of all individuals at different stages. However, there are no objective guidelines to determine the optimal number of classes. We used the following criteria to make a decision about the number of classes: (i) each class was designed to have a minimum amount of individuals, (ii) a large coefficient of similarity indicated that fairly homogeneous clusters were merged, whereas a small coefficient of similarity indicated that clusters containing quite dissimilar members were combined, and (iii) resulting clusters should represent distinct soil physical characteristics. We analyzed clusters using analysis of variance (ANOVA) and significant differences were tested with post hoc comparison via least significant difference (LSD) procedure (SPSS Professional Statistics, 1994).

#### 2.4. Characterization of soil materials

Soil materials were defined based on expert knowledge. We used texture, bulk density, and water content as indicators to distinguish between reworked loess and glacial till. Reworked loess (Irewlo<sub>xyzt</sub>) was characterized by

|                                |   |
|--------------------------------|---|
| texture <sub>xyzt</sub> :      | Texture at a geographic location $x$ and $y$ , depth $z$ in m, and time $t$ with:<br>sand content <53%<br>silt content $\geq$ 40%<br>no min., max., and/or range for clay content |
| bulkdensity <sub>xyzt</sub> :  | Bulk density at a geographic location $x$ and $y$ , depth $z$ in m, and time $t \geq 1.30$ and $< 1.6 \text{ Mg m}^{-3}$  |
| watercontent <sub>xyzt</sub> : | Water content at a geographic location $x$ and $y$ , depth $z$ in m, and time $t$ water content $\geq 0.17 \text{ m}^3 \text{ m}^{-3}$ .  |

Glacial till (Igtill<sub>xyzt</sub>) was characterized by the following:

|                                |   |
|--------------------------------|---|
| texture <sub>xyzt</sub> :      | Texture at a geographic location $x$ and $y$ , depth $z$ in m, and time $t$ with:<br>sand content $\geq$ 53%<br>silt content $\leq$ 50%<br>no min., max., and/or range for clay content |
| bulkdensity <sub>xyzt</sub> :  | Bulk density at a geographic location $x$ and $y$ , depth $z$ in m, and time $t \geq 1.60 \text{ Mg m}^{-3}$  |
| watercontent <sub>xyzt</sub> : | Water content at a geographic location $x$ and $y$ , depth $z$ in m, and time $t$ water content $< 0.17 \text{ m}^3 \text{ m}^{-3}$ .   |

We chose a threshold of  $0.17 \text{ m}^3 \text{ m}^{-3}$  for water content to distinguish reworked loess from glacial till material. According to Maidment (1993) and our measurements on representative soils showed field capacities of  $0.091\text{--}0.170 \text{ m}^3 \text{ m}^{-3}$  for glacial till and  $0.240\text{--}0.366 \text{ m}^3 \text{ m}^{-3}$  for reworked loess. Field capacity is a conservative measure representing the potential of water remaining in a soil 2 or 3 days after having been wetted with water and after free drainage is negligible. We used the actual soil water content measured in the field as indicator.

Typically, the top layer of soils is highly influenced by tillage operations (e.g. plowing) resulting in a compacted zone. Mixing of topsoil from lower horizons with deep tillage causes differences in texture along the soil profile and aggregate and structure disruption. We used the convex shape of CIPs up to a depth of 30 cm to define a topsoil layer. Subsoil layers were determined using the vertical point inflection method, which is described in detail in Grunwald et al. (2001).

For each layer of each cluster we calculated mean and standard deviation (S.D.) for sand, silt and clay content, bulk density, and water content. These soil attributes were used to characterize soil materials. Data were analyzed using ANOVA. Means comparisons were made with protected LSD procedure (SPSS Professional Statistics, 1994).

#### 2.5. Spatial distribution of soil materials

To visualize the spatial distribution of reworked loess and glacial till we created a three-dimensional soil layer model for our study area. We used 2D ordinary kriging to generate surfaces of layers. Volumes of layers were created with linear interpolation in the vertical direction between these surfaces. Spatial modeling was performed using Environmental Visualization System software (EVS, 1999; Huntington Beach, CA).

#### 2.6. Study area

The 2.73 ha study site is located on the University of Wisconsin–Madison Agricultural Research Station at Madison in southern Wisconsin, USA. Soils are formed in glacial till underlying loess, and are classified as fine, mixed, mesic Typic or Mollic Hapludalfs or Typic Argiudolls. Glacial till material is heterogeneous with texture ranging from sand, loamy sand to sandy loam, and is rich in gravel and/or stones. In contrast, the loess material is more homogeneous and dominated by silt. Topography is gently rolling with elevation ranging from 320 to 330 m and slope from  $0^\circ$  to  $10^\circ$ . Land use was alfalfa (*Medicago sativa*) for the past 3 years. Climate is temperate humid and soil moisture regime is udic. The study area contains a soil topo-sequence contained within a closed depression,

which is a representative component of the local landscape.

### 3. Results

#### 3.1. Relationship between cone index and soil attributes

Significant positive correlation between soil attributes, e.g. between silt and clay content with a correlation coefficient of 0.581, and negative correlation, e.g. between sand and water content with a correlation coefficient of  $-0.870$ , were encountered (Table 2). However, there were no significant correlations between sand, silt, clay content, bulk density, water content and CI (Table 2). Results indicate that for our data set no clear relationship between CI and soil attributes exist. However, when penetration and soil data are combined with landform element data, a much clearer pattern of soil material distribution emerges.

A cross-section from lower to upper hillslope showing CIPs, interpolated cone indices utilizing ordinary kriging, and soil attributes for selected profiles are shown in Fig. 2. Relative similar cone indices (1700–2200 kPa) were encountered in CIPs G–K on footslope and toeslope landscape positions (Table 1; Fig. 2). These cone indices were the integrative response to silt loam (sil) texture, bulk densities between 1.19 and 1.32  $\text{Mg m}^{-3}$ , and water contents between 0.182 and 0.218  $\text{m}^3 \text{m}^{-3}$  in Nos. 8–10 indicating reworked loess material. The same soil material is inferred by soil attributes in the upper CIP of A and C (compare Nos. 1, 2, 4, and 5).

On the summit, shoulder, and backslope landscape positions large cone indices ( $>4000$  kPa) occurred below a depth of 0.80 m in CIPs A–F. These cone indices were the response to loamy sand (ls) and sandy loam (sl) texture, large bulk densities ( $\geq 1.71 \text{ Mg m}^{-3}$ , Nos. 3 and 7), and small water content ( $\leq 0.116 \text{ m}^3 \text{m}^{-3}$ , Nos. 3 and 7) indicating the presence of glacial till material. On footslope and toeslope landscape positions large cone indices ( $>3500$  kPa) were measured at locations K and M below a depth of about 0.80 m, which were the integrative response to silt loam texture (Nos. 11, 14, and 15), bulk densities between 1.31 and 1.49  $\text{Mg m}^3$ , and large water contents between 0.208 and 0.218  $\text{m}^3 \text{m}^{-3}$  (Nos. 11, 14, and 15) indicating reworked loess material. In both cases it was a combination of soil attributes, which produced a similar CI signal, i.e., large cone indices were measured in response to glacial till and reworked loess. Supplementary landform element information was necessary to distinguish among soil materials. Based on the spatial distribution of all soil attribute data (not shown here), we found that below a depth of 0.80 m reworked loess was found only on toeslope and footslope landscape positions, whereas glacial till was found on backslope, shoulder, and summit positions.

#### 3.2. Combining cone index clusters and soil material information

We grouped penetrations utilizing a hierarchical cluster analysis and determined the optimal number of classes using the agglomeration schedule and dendrogram analysis. A summary of both outputs is given

Table 2

Correlation between soil attributes and CI (indicates correlation is significant at the 0.05 level (two-tailed))<sup>a</sup>

| Spearman's correlation coefficient | Sand content | Silt content  | Clay content  | Bulk density | Water content | Cone index |
|------------------------------------|--------------|---------------|---------------|--------------|---------------|------------|
| Sand content                       | 1.0          | $-0.874^{**}$ | $-0.866^{**}$ | 0.399        | $-0.870^{**}$ | 0.220      |
| Silt content                       |              | 1.0           | $0.581^{**}$  | $0.574^{**}$ | $-0.709^{**}$ | $-0.230$   |
| Clay content                       |              |               | 1.0           | $-0.282$     | $0.828^{**}$  | $-0.193$   |
| Bulk density                       |              |               |               | 1.0          | $-0.139$      | 0.193      |
| Water content                      |              |               |               |              | 1.0           | $-0.118$   |
| CI                                 |              |               |               |              |               | 1.0        |

<sup>a</sup> Number of records: 51.

\*\* Correlation is significant at the 0.01 level (two-tailed).



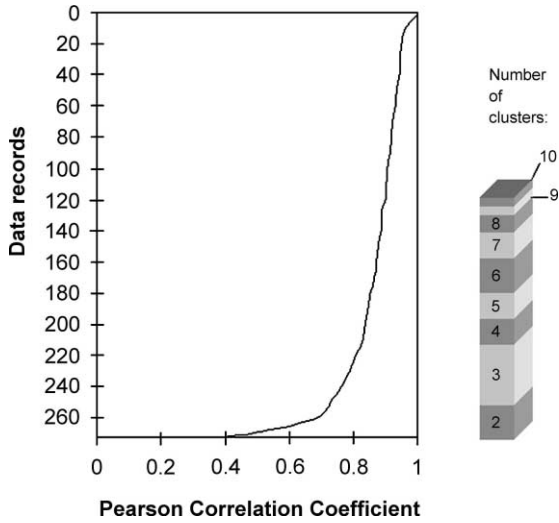


Fig. 3. The Pearson correlation coefficient and number of clusters computed by the hierarchical cluster analysis during the grouping process.

five landform element classes and contained the greatest number of CIPs ( $n$ : 202). The S.D. for sand content in layer 2 and clay, silt, sand, and water content in layer 3 of cluster B was extremely large (Table 4), expressing large variability of soil properties. These results were inconsistent with our definition for successful clustering, which states that clusters should represent distinctive physical soil characteristics.

We used our findings from Section 3.1 to subdivide cluster B into two groups based on landform element classes. Penetrations of cluster B encountered on backslope, shoulder, and summit landscape positions were grouped into group B1. Remaining penetrations encountered on toeslope and footslope landscape positions were grouped into group B2. We expected to find glacial till material in the bottom layer of group B1 and reworked loess material in the bottom layer of group B2.

Soil materials identified using texture, bulk density, and water content data are shown in Table 4. Significant differences between soil properties of layers within clusters are listed in Table 5. For example, layers 1 and 2 of cluster A differed significantly in sand content and bulk density, indicated by the asterisk (\*) symbol.

Layers 1 and 2 of cluster A corresponded to reworked loess, whereas layer 3 was glacial till. We found great differences in all soil properties except clay content between layers 2 and 3 of cluster A indicating a change in soil material. Layer 2 of cluster A had a wide variety of textures ranging from silt loam, silty clay loam, and clay loam to loam. Soil properties changed appreciably below 0.85 m depth with sand contents ranging from 68 to 92%, which corresponds to sandy loam, loamy sand and sand texture. The wide spread of S.D. around the mean CI penetration curve in layer 3 (Fig. 4) corresponded to large S.D. of sand content in layer 3 of cluster A (Table 4). Bulk density in layer 3 had a mean of  $1.71 \text{ Mg m}^{-3}$ , which is relatively large and in some soils would restrict root growth.

Layers 1 and 2 of cluster B correspond to reworked loess. Layer 3 of cluster B could not be clearly classified either as reworked loess or glacial till, because it showed a wide range of soil properties (Table 4). Subdividing cluster B into groups B1 and B2 improved soil material classification.

We found that B1 showed significantly different means for silt and water content between layers 1 and 2. Between layers 1 and 3 and between layers 2 and 3 of B1 all soil properties were significantly different (Table 5) indicating different soil materials. Soil texture in layers 1 and 2 of B1 was loam, silt loam, and silty clay loam indicating reworked loess, whereas in layer 3, we found loamy sand to sandy loam indicating glacial till (Table 4). Bulk densities and water contents confirmed our interpretation of

Table 3  
Thickness of layers in cm for clusters A–D

| Layer | Cluster A ( $n^a$ : 34) | Cluster B ( $n$ : 202) | Cluster C ( $n$ : 30) | Cluster D ( $n$ : 7) |
|-------|-------------------------|------------------------|-----------------------|----------------------|
| 1     | 0–30                    | 0–30                   | 0–30                  | 0–30                 |
| 2     | 30–85                   | 30–85                  | 30–130                | 30–130               |
| 3     | 85–130                  | 85–130                 | –                     | –                    |

<sup>a</sup> Number of penetration measurements.

| Depth (cm) | Clusters |     |       |       |
|------------|----------|-----|-------|-------|
|            | A        | B   | C     | D     |
| 0 - 3      |          |     |       |       |
| 3 - 6      |          |     |       |       |
| 6 - 9      |          |     |       |       |
| 9 - 12     | a        | b   | c     | a,b,c |
| 12 - 15    | a        | b   | c     | a,b,c |
| 15 - 18    | a        | b   | c     | a,b,c |
| 18 - 21    | a        | b   | c     | a,b,c |
| 21 - 24    | a        | b   | c     | a,b,c |
| 24 - 27    |          |     |       |       |
| 27 - 30    |          |     |       |       |
| 30 - 33    |          |     |       |       |
| 33 - 36    |          |     |       |       |
| 36 - 39    |          |     |       |       |
| 39 - 42    |          |     |       |       |
| 42 - 45    |          |     |       |       |
| 45 - 48    |          |     |       |       |
| 48 - 51    |          |     |       |       |
| 51 - 54    |          |     |       |       |
| 54 - 57    |          |     |       |       |
| 57 - 60    |          |     |       |       |
| 60 - 63    |          |     |       |       |
| 63 - 66    |          |     |       |       |
| 66 - 69    |          |     |       |       |
| 69 - 72    |          |     |       |       |
| 72 - 75    |          |     |       |       |
| 75 - 78    |          |     |       |       |
| 78 - 81    |          |     |       |       |
| 81 - 84    |          |     |       |       |
| 84 - 87    |          |     |       |       |
| 87 - 90    | a        |     | a     | a     |
| 90 - 93    | a        |     | a     | a     |
| 93 - 96    | a        |     | a     | a     |
| 96 - 99    | a        |     | a     | a     |
| 99 - 102   | a        | a   | a     | a     |
| 102 - 105  | a        | a,b | a     | a,b   |
| 105 - 108  | a        | a,b | a     | a,b   |
| 108 - 111  | a        | a,b | a,b   | a,b   |
| 111 - 114  | a        | a,b | a,b   | a,b   |
| 114 - 117  | a        | a,b | a,b,c | a,b,c |
| 117 - 120  | a        | a,b | a,b,c | a,b,c |
| 120 - 123  | a        | a,b | a,b,c | a,b,c |
| 123 - 126  | a        | a,b | a,b,c | a,b,c |
| 126 - 129  | a        | a,b | a,b   | a,b   |

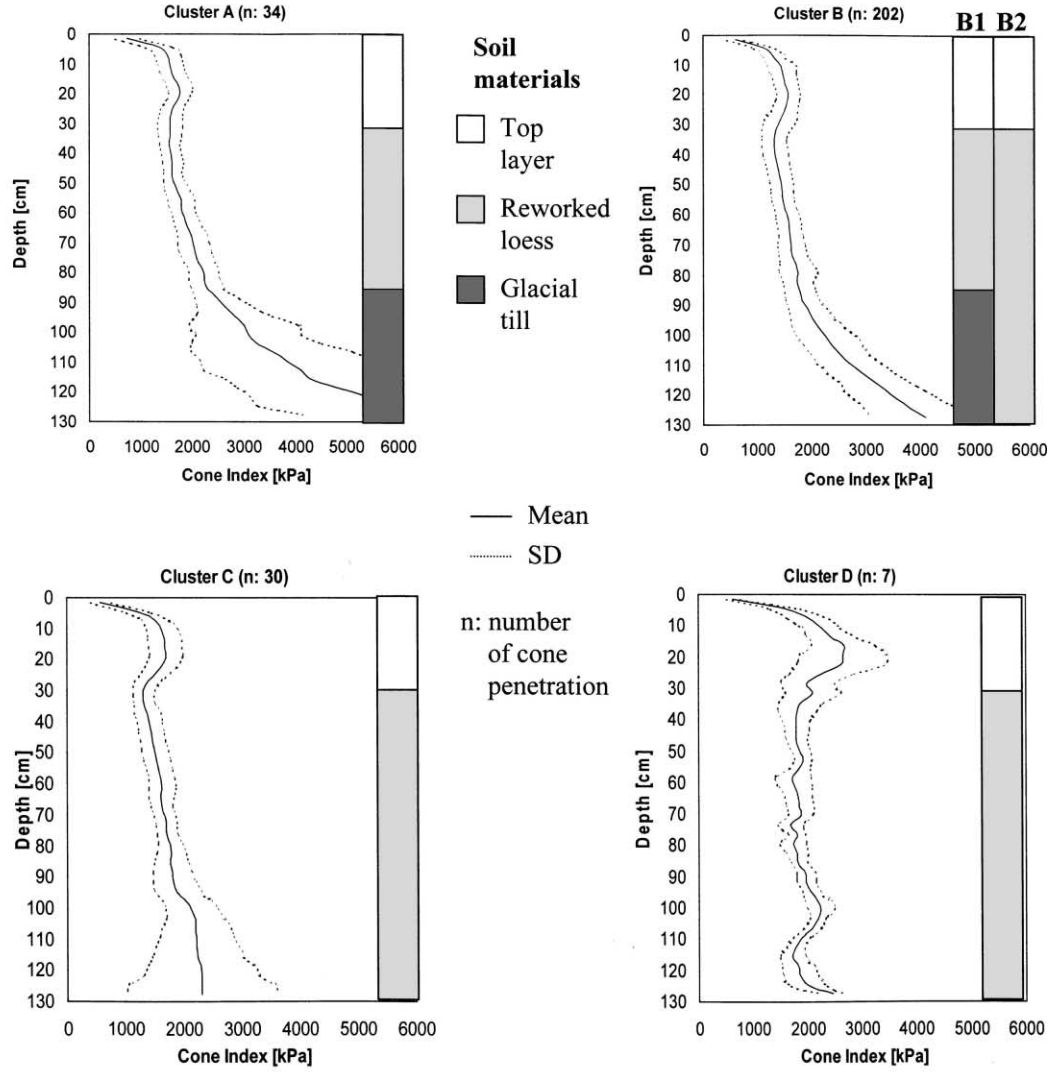


Fig. 4. CIPs and soil materials for cluster A–D. Depths where cone penetration resistance are significantly different at the 0.05 level are indicated with the same letter; those with no significant differences are not listed.

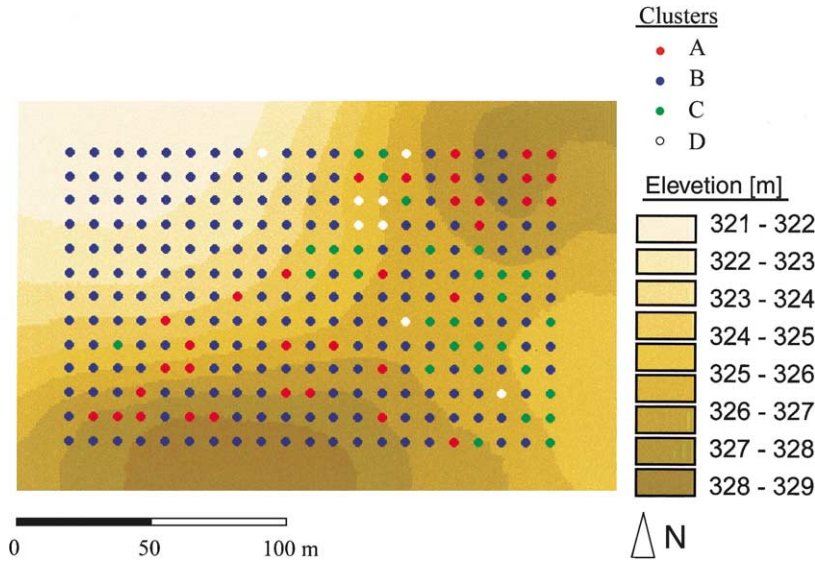


Fig. 5. DEM and spatial distribution of clusters across the study area.

different soil materials found in the two upper layers and layer 3.

Layers 1–3 of group B2 were classified as reworked loess, with sand content <53% and silt content ≥40%, bulk densities ≥1.30 and <1.6 Mg m<sup>-3</sup>, and water content ≥0.17 m<sup>3</sup> m<sup>-3</sup>. Texture in layer 1 of B2

was silt loam and in layers 2 and 3 silt loam and silty clay loam, respectively. The high mean bulk density of layer 3 cluster B2 might indicate a fragipan.

Layers 1 and 2 of cluster C differed greatly in terms of textural characteristics and bulk density (Table 4) though both layers were classified as reworked loess.

Table 4

Mean and S.D. for clay, silt and sand content, bulk density ( $\rho_b$ ) and soil volumetric water content ( $\theta$ ) for layers identified by the hierarchical cluster analysis (values in italics denote rework loess and values in bold denote glacial till)

| Layer | Attribute                                  | Cluster A                                | Cluster B           | Cluster B1          | Cluster B2          | Cluster C           | Cluster D           |
|-------|--|--|---------------------|---------------------|---------------------|---------------------|---------------------|
| 1     | Clay (%)                                   | <i>13.5<sup>a</sup>; 0.9<sup>b</sup></i> | <i>21.7; 1.4</i>    | <i>20.5; 1.2</i>    | <i>11.8; 0.6</i>    | <i>21.5; 1.4</i>    | <i>22.5; 0.6</i>    |
|       | Silt (%)                                   | <i>63.0; 1.9</i>                         | <i>59.5; 2.0</i>    | <i>58.6; 1.4</i>    | <i>60.3; 1.7</i>    | <i>58.3; 1.4</i>    | <i>65.5; 1.5</i>    |
|       | Sand (%)                                   | <i>22.1; 2.0</i>                         | <i>21.7; 1.9</i>    | <i>20.6; 1.4</i>    | <i>22.7; 1.8</i>    | <i>21.2; 2.4</i>    | <i>10.1; 1.0</i>    |
|       | $\rho_b$ (Mg m <sup>-3</sup> )             | <i>1.30; 0.12</i>                        | <i>1.39; 0.07</i>   | <i>1.45; 0.05</i>   | <i>1.32; 0.11</i>   | <i>1.60; 0.10</i>   | <i>1.71; 0.10</i>   |
|       | $\theta$ (m <sup>3</sup> m <sup>-3</sup> ) | <i>0.19; 0.012</i>                       | <i>0.188; 0.006</i> | <i>0.184; 0.006</i> | <i>0.192; 0.006</i> | <i>0.188; 0.007</i> | <i>0.194; 0.005</i> |
| 2     | Clay (%)                                   | <i>13.3; 1.0</i>                         | <i>21.6; 1.9</i>    | <i>20.7; 1.1</i>    | <i>22.5; 0.7</i>    | <i>26.0; 0.9</i>    | <i>24.3; 0.7</i>    |
|       | Silt (%)                                   | <i>62.1; 1.8</i>                         | <i>62.5; 2.0</i>    | <i>61.9; 1.1</i>    | <i>63.1; 0.9</i>    | <i>67.2; 1.1</i>    | <i>62.2; 1.5</i>    |
|       | Sand (%)                                   | <i>36.3; 7.9</i>                         | <i>15.7; 6.1</i>    | <i>20.3; 1.5</i>    | <i>11.1; 1.2</i>    | <i>12.1; 1.6</i>    | <i>11.2; 1.7</i>    |
|       | $\rho_b$ (Mg m <sup>-3</sup> )             | <i>1.38; 0.02</i>                        | <i>1.43; 0.09</i>   | <i>1.50; 0.07</i>   | <i>1.36; 0.05</i>   | <i>1.38; 0.13</i>   | <i>1.37; 0.05</i>   |
|       | $\theta$ (m <sup>3</sup> m <sup>-3</sup> ) | <i>0.198; 0.003</i>                      | <i>0.197; 0.006</i> | <i>0.200; 0.011</i> | <i>0.194; 0.012</i> | <i>0.197; 0.005</i> | <i>0.199; 0.004</i> |
| 3     | Clay (%)                                   | <b>9.1; 1.2</b>                          | 20.0; 15.1          | <b>10.3; 0.7</b>    | 30.0; 0.5           | –                   | –                   |
|       | Silt (%)                                   | <b>9.1; 1.0</b>                          | 36.3; 28.5          | <b>10.4; 1.2</b>    | 62.1; 0.7           | –                   | –                   |
|       | Sand (%)                                   | <b>80.5; 9.1</b>                         | 43.9; 35.0          | <b>79.0; 1.3</b>    | 8.8; 0.9            | –                   | –                   |
|       | $\rho_b$ (Mg m <sup>-3</sup> )             | <b>1.71; 0.05</b>                        | 1.58; 0.11          | <b>1.65; 0.07</b>   | 1.51; 0.10          | –                   | –                   |
|       | $\theta$ (m <sup>3</sup> m <sup>-3</sup> ) | <b>0.127; 0.006</b>                      | 0.169; 0.049        | <b>0.121; 0.012</b> | 0.217; 0.004        | –                   | –                   |

<sup>a</sup> Mean.

<sup>b</sup> S.D.

Table 5  
Significant different layers for clusters<sup>a</sup>

|                | Layer 1 |       |         |          |          | Layer 2 |       |         |          |          |
|----------------|---------|-------|---------|----------|----------|---------|-------|---------|----------|----------|
|                | cl      | si    | s       | $\rho_b$ | $\theta$ | cl      | si    | s       | $\rho_b$ | $\theta$ |
| <i>Layer 2</i> |         |       |         |          |          |         |       |         |          |          |
| cl             | b,c     |       |         |          |          |         |       |         |          |          |
| si             |         | c,d   |         |          |          |         |       |         |          |          |
| s              |         |       | b,c,e,f |          |          |         |       |         |          |          |
| $\rho_b$       |         |       |         | c,e,g    |          |         |       |         |          |          |
| $\theta$       |         |       |         |          | d,f      |         |       |         |          |          |
| <i>Layer 3</i> |         |       |         |          |          |         |       |         |          |          |
| cl             | b,d     |       |         |          |          | b,d     |       |         |          |          |
| si             |         | d,e,f |         |          |          |         | d,e,f |         |          |          |
| s              |         |       | b,d,e,f |          |          |         |       | b,d,e,f |          |          |
| $\rho_b$       |         |       |         | b,d,e,f  |          |         |       |         | b,d,e,f  |          |
| $\theta$       |         |       |         |          | d,e,f    |         |       |         |          | d,e,f    |

<sup>a</sup> cl: clay content in %; si: silt content in %; s: sand content in %;  $\rho_b$ : bulk density in  $Mg\ m^{-3}$ ;  $\theta$ : water content in  $m^3\ m^{-3}$ .

<sup>b</sup> Cluster B2.

<sup>c</sup> Cluster C.

<sup>d</sup> Cluster B1.

<sup>e</sup> Cluster A.

<sup>f</sup> Cluster B.

<sup>g</sup> Cluster D.

The CIP of cluster D was quite distinct from all other clusters (Fig. 4). We found large CI in layer 1, which corresponded to loam, silt loam, silty clay loam texture, and large mean bulk density with  $1.71\ Mg\ m^{-3}$

(Table 4). This might be a compacted layer caused by tillage. Mean bulk density was smaller in layer 2 of cluster D with  $1.37\ Mg\ m^{-3}$ . Bulk density was the only soil property that distinguished layer 1 from layer 2 of

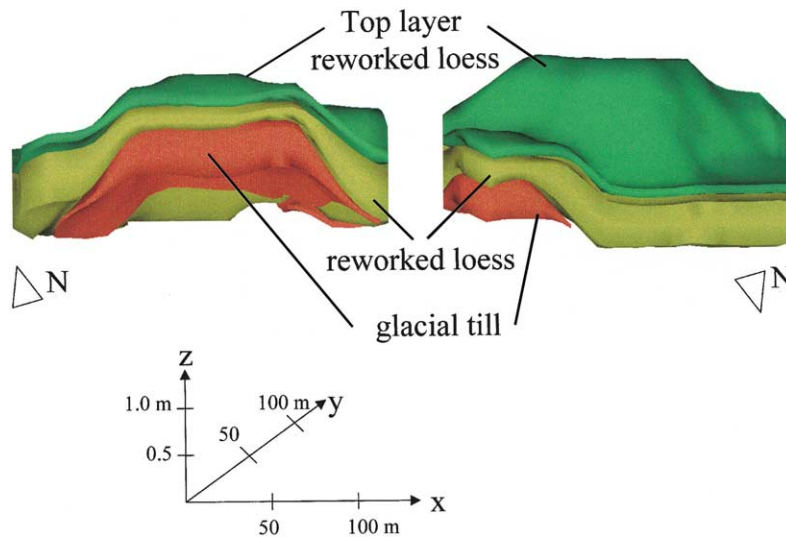


Fig. 6. Three-dimensional soil layer model showing the spatial distribution of soil materials.

cluster D (Table 5). Both layers of cluster D complied with criteria for reworked loess, except for the large bulk density found in layer 1.

The final step was to combine soil material information derived from the sparse soil attribute data set with the dense CI data set to derive a map showing the spatial distribution of soil materials across the entire study area. We created a three-dimensional soil material model (Fig. 6), which portrays the spatial distribution of soil materials. Layer 1 corresponded to a top layer formed in reworked loess and highly influenced by tillage. Shallow reworked loess cover was found on eroded soils on shoulder and backslope positions, whereas thick reworked loess deposits occurred on footslope and toeslope positions. Glacial till occurred close to the surface on higher elevated areas while no glacial till was found in the depression up to a depth of 1.3 m. Distribution of soil materials was closely associated with topographic attributes.

#### 4. Discussion

In this study, we presented a heuristic approach using a working hypothesis about the spatial distribution of soil materials. We utilized penetration resistance measurements to map two contrasting soil materials, glacial till and reworked loess, where experts characterized soil materials based on soil-factor combinations of texture, bulk density, and water content. Our hypothesis was drawn in analogy to other studies in which authors utilized penetration resistance measurements comparing different tillage practices (Hilfiker and Lowery, 1988; Unger, 1996; Tessier et al., 1997). These studies assumed that penetration resistance is the measured response to soil-factor combinations while tillage systems affect specific soil properties differently. For example, zero tillage, conservation, and conventional tillage differ in their impact on aggregate stability, compaction, water holding capacity, and organic matter content.

Other authors focus on the relationship between soil attributes and penetration resistance. These studies are often limited to uniform, however, disturbed soils, either sands (Kasim et al., 1986; Puppala et al., 1995) or fine clays (Levadoux and Baligh, 1986; Sully and Campanella, 1991) or a given soil type, where penetration resistance is related to quantitative soil

properties such as water content (Vepraskas, 1984). These tests limit the evaluation of the relative effect of one specific compositional variable (such as texture) or environmental variable (such as water content) on penetration resistance. In our study such an approach did not produce conclusive results indicated by very small correlations between soil attributes and CI.

Results of this study suggest that CI measurements at specific geographic locations corresponding to landform classes were related to soil-factor combinations. These soil-factor combinations characterize soil materials. Identifying reworked loess and glacial till utilizing cone indices is associated with uncertainty. We calculated S.D. for soil attributes (Table 4) and for cone indices of clusters (Fig. 4) to express uncertainty associated with soil material identification.

Soil material characterization by experts used crisp boundaries of  $1.60 \text{ Mg m}^{-3}$  for bulk density and  $0.17 \text{ m}^3 \text{ m}^{-3}$  for water content. Reworked loess contained loam, clay loam, silty clay, silty clay loam, silt loam, and silt texture, whereas glacial till was associated with sandy clay, sandy clay loam, sandy loam, loamy sand, and sand texture classes. Soil materials with distinct differences in soil properties such as reworked loess and glacial till deposits can be easily mapped with a PCP at landscape-scale. However, in landscapes with similar soil materials such an approach might fail to identify changes in soil material distribution.

Glacial till and loess impart major control on crop growth and yield as well as the transport of agrichemicals. Stratigraphic details help us to more clearly understand a landscape. Soil material models are beneficial for land management and environmental assessment studies. A more comprehensive study is in preparation to verify our methodology developed for soil material mapping.

#### 5. Summary and conclusion

The objective of this study was to distinguish among soil materials found in a glaciated landscape in southern Wisconsin, USA. We used a dense data set of cone penetrations, a sparse data set of laboratory measured soil properties, and landform element classes to accomplish our goal. Thus, we combined rapid sampling techniques with cost-intensive and

labor-intensive procedures. However, this method is associated with large uncertainties in some areas and can be recommended only for coarse mapping of contrasting soil materials at landscape-scale. Results indicated that combined information consisting of CI and geographic location information improved soil material mapping. This points in the direction using supplementary information such as sleeve resistance measurements or soil imaging penetrometers to reliably identify soil materials.

## References

- ArcView, 1999. Environmental Systems Research Institute, Inc., Redlands, CA. <http://www.esri.com/>.
- Assallay, A.M., Jefferson, I., Rogers, C.D.F., Smalley, I.J., 1998. Fragipan formation in loess soils: development of the Bryant hydroconsolidation hypothesis. *Geoderma* 83, 1–16.
- Awadhwai, N.K., Smith, G.D., 1990. Performance of low-draft tillage implements on a hard setting Alfisol of the SAT in India. *Soil Use Manage.* 6, 28–31.
- Ayers, P.D., Perumpral, J.V., 1982. Moisture and density effect on cone index. *Trans. ASAE* 25 (5), 1169–1172.
- Bar-Josef, B., Lambert, J.R., 1981. Corn and cotton root growth response to soil impedance and water potential. *Soil Sci. Soc. Am. J.* 45, 930–935.
- Beven, K.J., Moore, I.D., 1993. *Terrain Analysis and Distributed Modeling in Hydrology. Advances in Hydrological Processes.* Wiley, Chichester, UK.
- Bowen, H.D., 1976. Correlations of penetrometer cone index with root impedance. *Am. Soc. Agric. Eng. (St. Joseph)* 76, 1516–1522.
- EVS (Environmental Visualization System), 1999. Ctech Development Corporation, Huntington Beach, CA. <http://www.ctech.com/>.
- Faure, A.G., Da Mata, J.D.V., 1994. Penetration resistance value among compaction curves. *J. Geotech. Eng.* 120 (1), 46–59.
- Grunwald, S., Rooney, D.J., McSweeney, K., Lowery, B., 2001. Development of pedotransfer functions for a profile cone penetrometer. *Geoderma* 100, 25–47.
- Hilfiker, R.E., Lowery, B., 1988. Effect of conservation tillage systems on corn root growth. *Soil Till. Res.* 12, 269–283.
- Huggett, R.J., 1975. Soil landscape systems: a model of soil genesis. *Geoderma* 13, 1–22.
- Kasim, A.G., Chu, M.-Y., Jensen, C.N., 1986. Field correlation of cone and standard penetration tests. *J. Geotech. Eng.* 112 (3), 368–372.
- Kurup, P.U., Voyiadjis, G.Z., Tumay, M.T., 1994. Calibration chamber studies of piezocone test in cohesive soils. *J. Geotech. Eng.* 120 (1), 81–107.
- Laboski, C.A.M., Dowdy, R.H., Allmaras, R.R., Lamb, J.A., 1998. Soil strength and water content influences on corn root distribution in a sandy soil. *Plant and Soil* 203, 239–247.
- Levadoux, J.-N., Baligh, M.M., 1986. Consolidation after undrained peizocone penetration. I. Prediction. *J. Geotech. Eng.* 112 (7), 707–726.
- Lowery, B., Schuler, R.T., 1994. Duration and effects of compaction on soil and plant growth in Wisconsin. *Soil Till. Res.* 29, 205–210.
- Maidment, D.R., 1993. *Handbook of Hydrology.* McGraw-Hill, New York.
- Materechera, S.A., Mloza-Banda, H.R., 1997. Soil penetration resistance, root growth and yield of maize as influenced by tillage system on ridges in Malawi. *Soil Till. Res.* 41, 13–24.
- Pikul Jr., J.L., Aase, J.K., 1999. Wheat response and residual soil properties following subsoiling of a sandy loam in eastern Montana. *Soil Till. Res.* 51, 61–70.
- Puppala, A.J., Acar, Y.B., Tumay, M.T., 1995. Cone penetration in very weakly cemented sand. *J. Geotech. Eng.* 121 (8), 589–600.
- Rooney, D.J., Lowery, B., 2000. A profile cone penetrometer (PCP) for mapping soil horizons. *Soil Sci. Soc. Am. J.* 64 (6), 2136–2139.
- SPSS Professional Statistics, 1994. *User's Manual for SPSS Statistical Software Package.* SPSS, Chicago, IL.
- Sully, J.P., Campanella, R.G., 1991. Effect of lateral stress on CPT penetration pore pressures. *J. Geotech. Eng.* 117 (7), 1082–1088.
- Taboada, M.A., Micucci, F.G., Cosentino, D.J., Lavado, R.S., 1998. Comparison of compaction induced by conventional and zero tillage in two soils of the Rolling Pampa of Argentina. *Soil Till. Res.* 49, 57–63.
- Tessier, S., Lachance, B., Chen, Y., Chi, L., Bachand, D., 1997. Soil compaction reduction with modified one-way disk. *Soil Till. Res.* 42, 63–77.
- Trimble, 1996. Trimble Navigation Europe Ltd. Differential GPS 4000 Series. Sunnyvale, CA.
- Trouse Jr., A.C., 1983. Observation on under the row subsoiling after conventional tillage. *Soil Till. Res.* 3 (1), 67–81.
- Unger, P.W., 1996. Soil bulk density, penetration resistance, and hydraulic conductivity under controlled traffic conditions. *Soil Till. Res.* 37, 67–75.
- Vepraskas, M.J., 1984. Cone index of loamy sands as influenced by pore size distribution and effective stress. *Soil Sci. Soc. Am. J.* 48, 1220–1225.
- Voorhees, W.B., 1987. Assessment of soil susceptibility to compaction using soil and climate databases. *Soil Till. Res.* 10 (1), 29–38.